

Electron scattering, charge order, and pseudogap physics in $\text{La}_{1.6-x}\text{Nd}_{0.4}\text{Sr}_x\text{CuO}_4$: An angle-resolved photoemission spectroscopy study

C. E. Matt,^{1,2} C. G. Fatuzzo,³ Y. Sassa,^{1,2,4} M. Måansson,^{3,5,6} S. Fatale,³ V. Bitetta,³ X. Shi,¹ S. Pailhès,^{6,7} M. H. Berntsen,⁵ T. Kurosawa,⁸ M. Oda,⁸ N. Momono,⁹ O. J. Lipscombe,¹⁰ S. M. Hayden,¹⁰ J.-Q. Yan,¹¹ J.-S. Zhou,¹² J. B. Goodenough,¹² S. Pyon,¹³ T. Takayama,¹³ H. Takagi,¹³ L. Patthey,¹ A. Bendounan,¹ E. Razzoli,^{1,14} M. Shi,¹ N. C. Plumb,¹ M. Radovic,¹ M. Grioni,³ J. Mesot,^{2,3,6} O. Tjernberg,^{5,15} and J. Chang^{1,3,16}

¹Swiss Light Source, Paul Scherrer Institut, CH-5232 Villigen PSI, Switzerland

²Laboratory for Solid State Physics, ETH Zürich, CH-8093 Zürich, Switzerland

³Institute for Condensed Matter Physics, École Polytechnique Fédérale de Lausanne (EPFL), CH-1015 Lausanne, Switzerland

⁴Department of Physics and Astronomy, Uppsala University, S-75121 Uppsala, Sweden

⁵KTH Royal Institute of Technology, Materials Physics, S-164 40 Kista, Sweden

⁶Laboratory for Neutron Scattering, Paul Scherrer Institut, CH-5232 Villigen, Switzerland

⁷Institut Lumière Matière, UMR5306 Université Lyon 1-CNRS, Université de Lyon, 69622 Villeurbanne, France

⁸Department of Physics, Hokkaido University - Sapporo 060-0810, Japan

⁹Department of Applied Sciences, Muroran Institute of Technology, Muroran 050-8585, Japan

¹⁰H. H. Wills Physics Laboratory, University of Bristol, Bristol BS8 ITL, United Kingdom

¹¹Materials Science and Technology Division, Oak Ridge National Laboratory, Oak Ridge, Tennessee 37831, USA

¹²Texas Materials Institute, University of Texas at Austin, Austin, Texas 78712, USA

¹³Department of Advanced Materials, University of Tokyo, Kashiwa 277-8561, Japan

¹⁴Département de Physique and Fribourg Center for Nanomaterials, Université de Fribourg, CH-1700 Fribourg, Switzerland

¹⁵Center for Quantum Materials, KTH Royal Institute of Technology, and Stockholm University,

Roslagstullsbacken 23, S-106 91 Stockholm, Sweden

¹⁶Physik-Institut, Universität Zürich, Winterthurerstrasse 190, CH-8057 Zürich, Switzerland

(Received 7 August 2014; revised manuscript received 24 August 2015; published 27 October 2015)

We report an angle-resolved photoemission study of the charge stripe ordered $\text{La}_{1.6-x}\text{Nd}_{0.4}\text{Sr}_x\text{CuO}_4$ (Nd-LSCO) system. A comparative and quantitative line-shape analysis is presented as the system evolves from the overdoped regime into the charge ordered phase. On the overdoped side ($x = 0.20$), a normal-state antinodal spectral gap opens upon cooling below 80 K. In this process, spectral weight is preserved but redistributed to larger energies. A correlation between this spectral gap and electron scattering is found. A different line shape is observed in the antinodal region of charge ordered Nd-LSCO $x = 1/8$. Significant low-energy spectral weight appears to be lost. These observations are discussed in terms of spectral-weight redistribution and gapping originating from charge stripe ordering.

DOI: 10.1103/PhysRevB.92.134524

PACS number(s): 74.25.Jb, 74.72.Gh, 74.72.Kf

I. INTRODUCTION

Partial gapping of spectral weight in the absence of any metal instability appears in many strongly correlated electron systems [1–4]. This so-called pseudogap phenomenon is, for example, found in the normal state of charge-density-wave (CDW) systems, above the CDW onset temperature [5]. A pseudogap phase has also been reported in the normal state of high-temperature cuprate superconductors. The nature of these pseudogaps is still being debated [6–15]. Recently, it has become clear that charge ordering is a universal property of hole-doped cuprates [16–30]. Around the so-called 1/8 doping, the CDW onset temperature appears much before the superconducting transition temperature. The normal state of cuprates should hence be revisited to identify a single-particle gap from CDW order and to investigate the spectral gapping in the absence of both superconductivity and CDW order. We therefore present an angle-resolved photoemission spectroscopy (ARPES) study of the well-known charge stripe ordered system $\text{La}_{1.6-x}\text{Nd}_{0.4}\text{Sr}_x\text{CuO}_4$ (Nd-LSCO), in which charge and spin orders are coupled [31,32]. As shown in the phase diagram (Fig. 1), this material has a strongly suppressed superconducting transition temperature, which allows a low-temperature study of the normal state. We have studied the spectral

line-shape evolution as a function of momentum, temperature, and doping. On the overdoped side, Nd-LSCO $p = 0.20$, an antinodal spectral gap is observed. This gap can be closed by either increasing doping to $p = 0.24$, increasing temperature to $T \sim 80$ K, or moving in momentum towards the zone diagonal. The normal-state gap Δ redistributes spectral weight up to $\sim 2.5\Delta$, but the total weight remains conserved. Analysis of the spectral line shape suggests a correlation between the gap amplitude and electron scattering. In the underdoped regime $p < 0.15$, the antinodal line shape changes. Compared to the overdoped side of the phase diagram, a significant suppression of spectral weight is observed. This effect is discussed in terms of quasiparticle decoherence and competing orders. In particular, the idea that charge stripe order can contribute to the suppression of antinodal spectral weight is discussed.

II. METHODS

Our ARPES experiments were carried out at the Swiss Light Source (SLS) on the Surface and Interface Spectroscopy (SIS) beam line, [33] using 55 eV circular polarized photons. Single crystals of Nd-LSCO with $x = p = 0.12, 0.15, 0.20$, and 0.24—grown by the traveling-zone method—were cleaved *in situ* under ultrahigh-vacuum (UHV) conditions ($\sim 0.5 \times$

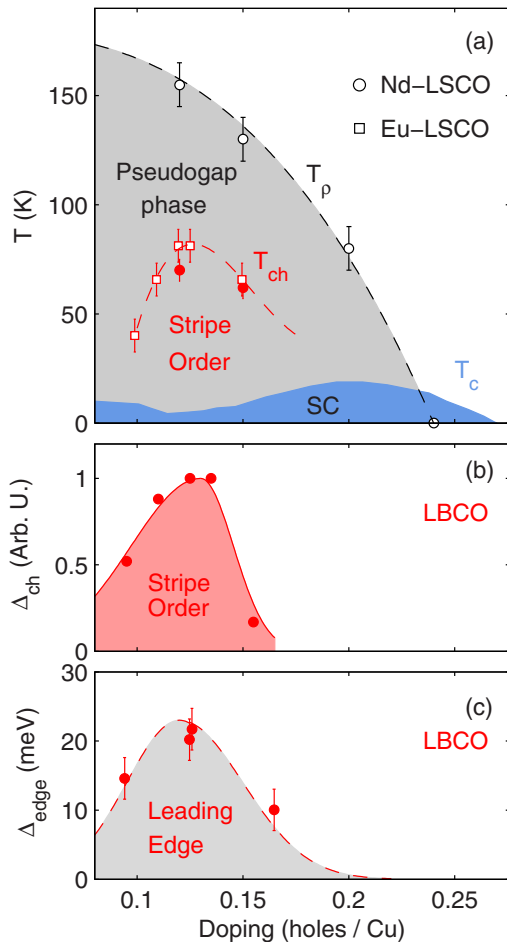


FIG. 1. (Color online) (a) Temperature-doping phase diagram of $\text{La}_{1.6-x}\text{Nd}_{0.4}\text{Sr}_x\text{CuO}_4$ (Nd-LSCO), established by diffraction and resistivity experiments [31,34–37]. The temperature scale T_p is determined by the deviation from high-temperature linear resistivity [34]. The charge ordering temperature (T_{ch}) is obtained from x-ray diffraction [31,36,37]. All lines are guides to the eye. (b) Charge stripe order parameter Δ_{ch} , derived from hard x-ray diffraction experiments on $\text{La}_{2-x}\text{Ba}_x\text{CuO}_4$ (LBCO) [38]. (c) Leading edge gap of LBCO vs doping, from Ref. [39].

10^{-10} mbar) using a top-post technique or a specially designed cleaving tool [40]. Photoemitted electrons were analyzed using a SCIENTA 2002 or a R4000 analyzer. A total-energy resolution of ~ 15 meV was achieved with this setup. Due to matrix element effects, all data were recorded in the second Brillouin zone but represented by the equivalent points in the first zone. The Fermi level was measured on polycrystalline copper in thermal and electric contact with the sample. Copper spectra were also used to normalize detector efficiencies.

III. RESULTS

Normal-state ($T \gtrsim T_c$) energy-distribution maps taken in the antinodal $(\pi, 0)$ region of Nd-LSCO $x = p = 0.12, 0.15, 0.20$, and 0.24 are shown in Fig. 2. As doping p is reduced, the “quasiparticle” excitations are gradually broadened. Finite spectral weight at the Fermi level E_F ($\omega = 0$) is, however, found for all compositions even deep inside the charge stripe ordered phase [41]. It is thus possible to define the underlying

Fermi momenta k_F from the maximum intensity of the momentum distribution curves (MDCs) at $\omega = 0$. The Nd-LSCO Fermi surface topology [42], shown schematically in Fig. 2, is similar to that of $\text{La}_{2-x}\text{Sr}_x\text{CuO}_4$ (LSCO) [43,44] and $\text{Bi}_2\text{Sr}_2\text{CaCu}_2\text{O}_{8+x}$ (Bi2212) [45,46]. A van Hove singularity crosses E_F at a doping concentration slightly larger than $x = p = 0.20$, separating electron- from hole-like Fermi surfaces.

A. Spectral line shapes

The analysis of symmetrized energy-distribution curves (EDCs) at $k = k_F$ is a standard method to visualize the existence of a spectral gap near the Fermi level [47]. A single-particle gap shifts the spectral weight away from the Fermi level and hence produces a double-peak structure in the symmetrized curves. In the absence of a spectral gap, the symmetrized EDC at k_F is, on the contrary, characterized by a line shape peaked at the Fermi level.

For overdoped LSCO and Nd-LSCO $p \sim 0.24$, the antinodal spectra have a Voigt-like profile [see top spectrum of Figs. 3(a) and 3(b)] just above T_c , suggesting resolution-limited gapless excitations. At slightly lower doping in Nd-LSCO $p = 0.20$, a clear spectral gap $\Delta \sim 25$ – 30 meV is found in the antinodal region for $T \sim T_c$ [Fig. 3(b)]. Similar line shapes of the ARPES spectra were obtained on Nd-LSCO $p \sim 0.15$ and LSCO with $p = 0.105, 0.12$, and 0.15 ; see Figs. 3(a) and 3(b). As in Bi2212 and $\text{Bi}_2\text{Sr}_2\text{CuO}_{6+x}$ (Bi2201) [48–50], a dramatic change of antinodal line shape appears for underdoped Nd-LSCO [Fig. 3(b)]. The peaked line-shape structure—found for Nd-LSCO $p = 0.15$ and 0.20 —is strongly depleted.

A similar evolution of the line shape is found when moving from the antinodal to the nodal region in Nd-LSCO at $p = 0.12$ [Fig. 3(c)]. It resembles the doping dependence [Fig. 3(b)]: first the double-peaked structure is recovered, and second, upon entering the Fermi arc, gapless excitations are found [41]. For comparison, the momentum dependence of the EDC line shapes in Nd-LSCO $p = 0.20$ is shown in Fig. 3(d). At this doping, a peaked structure is found for all underlying Fermi momenta [see Fig. 3(d)]. The temperature dependence of antinodal spectra is also very different in Nd-LSCO $p = 0.12$ and 0.20 —see Figs. 3(e), 3(f), and 4. For $p = 0.20$, the normal-state gap closes at $T \approx 80$ K, while it persists in the stripe order $p = 0.12$ compound. Furthermore, the peaked structure in the symmetrized EDC line shape becomes more pronounced in $p = 0.20$ upon cooling [Fig. 3(f)]. The opposite trend is observed at 0.12 doping. In fact, as in Bi2201 [48], a much sharper antinodal line shape is found at 75 K compared to 17 K. Finally, the spectral gap in $p = 0.20$ seems to conserve but redistribute the spectral weight (Fig. 4) as it opens upon cooling. In contrast, for underdoped Nd-LSCO $p = 0.12$, spectral weight is either lost or redistributed in a nontrivial fashion upon cooling. The antinodal spectra at the anomalous $1/8$ doping are thus behaving very differently from what is found in more overdoped samples of Nd-LSCO. The $1/8$ antinodal spectra are also very different from what is observed in LSCO at similar doping (Fig. 3).

B. Background subtraction

The raw spectra, described above, are composed of an intrinsic signal on top of an extrinsic background. Importantly,

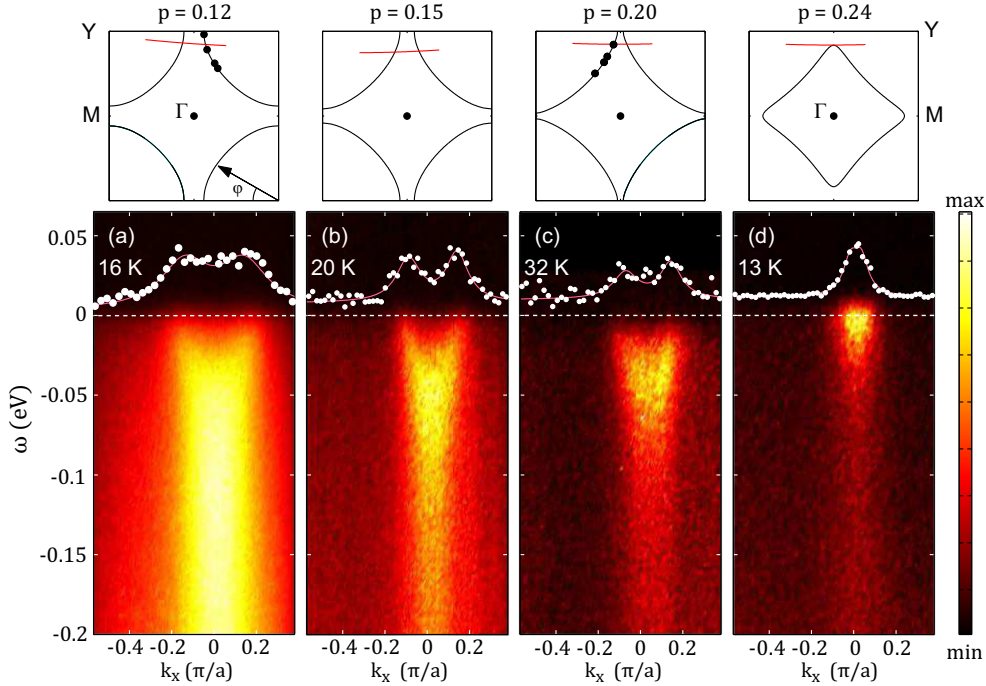


FIG. 2. (Color online) (a)–(d) Antinodal angle-resolved photoemission spectra, taken in the normal state of $\text{La}_{1.6-x}\text{Nd}_{0.4}\text{Sr}_x\text{CuO}_4$ for different dopings $p = x$ as indicated. Solid white points are momentum distribution curves at the Fermi level, indicated by horizontal dashed lines. Top panels schematically show the Fermi-surface topology for each of the doping concentrations. The red lines indicate the trajectory along which the antinodal spectra were recorded. Solid black points indicate the underlying Fermi momenta at which symmetrized EDCs are shown in Figs. 3(c) and 3(d).

the extrinsic background has essentially the same profile for all measured compounds. It is therefore possible to normalize spectral intensities relative to the extrinsic background—see the Appendix. Antinodal spectra were recorded on several cleaved surfaces of Nd-LSCO $p = 0.12$ and different ratios between signal and extrinsic backgrounds were found. As a consequence, slightly different raw antinodal line shapes were extracted. However, once background was subtracted, consistent line shapes were reproduced (shown in the Appendix). As shown in Figs. 3(g)–3(l), only the antinodal line shape of Nd-LSCO with $p = 0.12$ is significantly influenced by the background subtraction. For all other spectra, the background subtraction has little impact on the overall line shape. In fact, for Nd-LSCO $p = 0.12$, the signal is comparable to the background, whereas for compounds with $p > 0.15$, the signal-to-background ratio is much larger (see Fig. 4). Again, this is an indication that the 1/8 antinodal spectra are anomalous.

IV. DISCUSSION

A. Line-shape modeling

Let us start by discussing the spectra on the overdoped side of the phase diagram. Neglecting matrix element effects, the symmetrized intensity $I(k_F, \omega)$ is given by the spectral function [47]

$$A(k_F, \omega) \sim -\text{Im}\Sigma/[(\omega - \text{Re}\Sigma)^2 + \text{Im}\Sigma^2]. \quad (1)$$

In the absence of a spectral gap, $\text{Re}\Sigma = 0$ at $k = k_F$ and the spectral function is nothing but a Lorentzian function,

when approximating $\text{Im}\Sigma$ by a constant Γ . If $\text{Im}\Sigma = \Gamma$ is comparable to the applied energy resolution, a Voigt line shape is effectively observed. This is the case for antinodal spectra of Nd-LSCO $p = 0.24$ [Fig. 3(h)]. The intrinsic linewidth Γ is a measure of the “quasiparticle” scattering. With increasing scattering, the line width broadens (Γ increases) and, assuming that spectral weight is conserved, the peak amplitude is lowered. In this fashion, a metal can lose its coherence.

In the presence of a spectral gap, Eliashberg theory applied to the normal state finds the Green’s function $G(k_F, \omega) = [(\omega + i\Gamma) - \Delta^2/(\omega + i\Gamma)]^{-1}$ to be given by two parameters: the gap Δ and the scattering rate Γ [57]. This functional form roughly mimics the observed line shape, but does not provide a fulfilling description of the experimental spectra. We, therefore, adopted a simpler phenomenological Green’s function, $G(k_F, \omega) = [(\omega + i\Gamma) - \Delta^2/\omega]^{-1}$, that contains the same two parameters and has previously been used to analyze symmetrized energy-distribution curves [8,51,52,58–60]. The spectral function $A(k_F, \omega) = \pi^{-1}\text{Im}G(k_F, \omega)$ can now be expressed by two dimensionless quantities,

$$A(x) \sim \frac{1}{\Delta} \frac{\gamma}{(x - 1/x)^2 + \gamma^2}, \quad (2)$$

where $x = \omega/\Delta$ and $\gamma = \Gamma/\Delta$. This phenomenological spectral function preserves the Lorentzian line shape and total spectral weight, but shifts the peaks to $x = \pm 1$ ($\omega = \pm\Delta$) while the linewidth Γ/Δ is renormalized by the spectral gap. For a fixed gap Δ , increasing quasiparticle scattering still leads

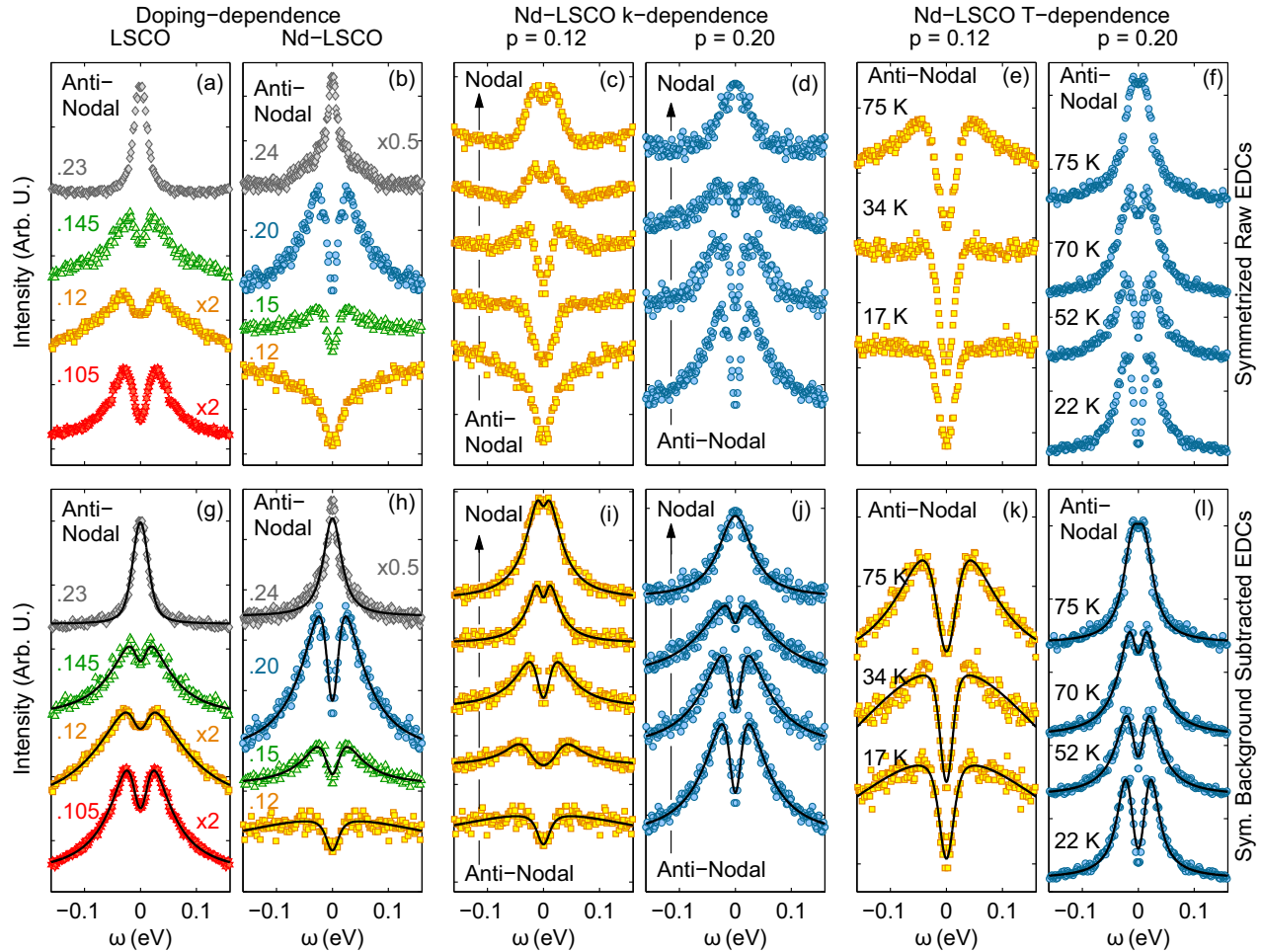


FIG. 3. (Color online) Symmetrized normal-state energy-distribution curves (EDCs) recorded on $\text{La}_{2-x}\text{Sr}_x\text{CuO}_4$ (LSCO) and $\text{La}_{1.6-x}\text{Nd}_{0.4}\text{Sr}_x\text{CuO}_4$ (Nd-LSCO). All spectra were taken just above T_c . (a)–(f) Raw symmetrized spectra; (g)–(l) background-subtracted spectra. (a), (b) Symmetrized EDCs taken in the antinodal region, for doping concentrations of LSCO and Nd-LSCO as indicated. ARPES data on LSCO $x = 0.105$ and 0.145 were previously presented in Refs. [51–53] and all LSCO samples were characterized by neutron-scattering experiments [54–56]. (c), (d) Momentum dependence of symmetrized energy-distribution curves (EDCs) taken at k_F moving from antinodal (bottom) to nodal (top) region for Nd-LSCO $p = 0.12$ and 0.20 . (e), (f) Temperature dependence of antinodal symmetrized EDCs recorded on Nd-LSCO $p = 0.12$ and 0.20 . For clarity, each spectrum has been given an arbitrary vertical shift. Solid lines in bottom panels are fits; see text for an explanation.

to a broader line and weaker peak amplitude. The absence of a peaked structure may therefore be a signature of strong quasiparticle scattering.

B. Spectral gap and scattering

Using Eq. (2), an analysis of background-subtracted spectra [61,62] was carried out. Resolution effects are modeled by Gaussian convolution of the model function $A(k_F, \omega)$ [Eqs. (1) and (2)]. In this fashion, Γ and Δ were extracted along the underlying Fermi surface of Nd-LSCO $p = 0.20$. As shown in Fig. 5, a correlation between the gap Δ and the scattering rate Γ is found. A similar trend is observed when the gap Δ is weakened by increasing temperature in Nd-LSCO $p = 0.20$. This relation between the antinodal gap (usually referred to as the pseudogap) and electron scattering is consistent with previous observations. It is, for example, established that the pseudogap is largest near the zone boundary [7,11,47]. At the same

time, the scattering rate Γ has been shown to increase when moving from nodal to antinodal regions [63,64]. Furthermore, the photoemission line shape broadens and the pseudogap increases when doping is reduced from the overdoped side of the phase diagram [49]. The same trend has been reported by scanning tunneling microscopy studies of the density of states [65,66]. The exact experimental relation between scattering and the pseudogap (normal-state gap) has, however, not been discussed much [67]. A correlation between scattering and the spectral gap has previously been predicted by dynamical mean-field theory (DMFT) calculations for the Hubbard model [68]. Within the DMFT approach [69–72], the pseudogap emerges from electron correlations as a primary effect that, in turn, enhances the tendency for the system to undergo superconducting and charge-density-wave instabilities, at lower temperatures. Notice, however, that opposed to superconductivity, charge order has not yet been found directly in DMFT calculations.

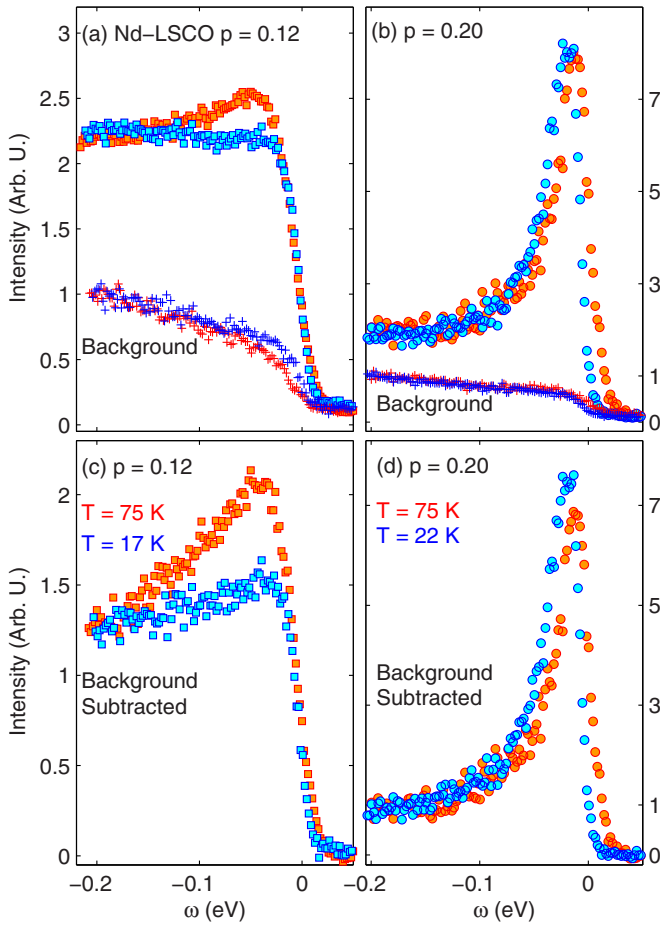


FIG. 4. (Color online) Comparison of antinodal spectra at $T \sim 20\text{ K}$ (blue) and 75 K (red). (a),(b) Raw energy-distribution curves recorded at k_F on Nd-LSCO $p = 0.12$ and 0.20 with the respective background intensities, measured at momenta far from k_F . (c),(d) The respective background-subtracted curves are compared.

From a different point of view, the pseudogap (normal-state gap) emerges as a precursor to superconductivity [7,8,73], or as a precursor to an order competing with superconductivity [26,48,74–76]. In Bi2201, for example, the charge ordering onset temperature is comparable to the pseudogap temperature scale T^* [26]. Furthermore, a connection between the charge ordering vector and the vector nesting the Fermi arc tips was found [26]. It is therefore a possibility that the pseudogap is related to fluctuating CDW order [77,78]. In two-dimensional CDW systems, spectral gaps are indeed observed above the CDW onset temperature [79,80]. In cuprates, however, the single-particle gap originating from CDW order has not been clearly elucidated by ARPES experiments.

C. Spectra gaps at 1/8 doping

It is therefore interesting to discuss the spectral line shapes at the 1/8 doping, where the charge order parameter has its maximum (Fig. 1). Charge order—in principle—should open a single-particle gap somewhere on the Fermi surface [80,82]. It is commonly assumed that the stripe ordered ground state found in Nd-LSCO is identical to that of $\text{La}_{2-x}\text{Ba}_x\text{CuO}_4$ (LBCO) and $\text{La}_{1.8-x}\text{Eu}_{0.2}\text{Sr}_x\text{CuO}_4$ (Eu-LSCO) with $p = x \simeq 1/8$ [83]. All three systems have the same low-temperature tetragonal crystal structure, similar thermopower [84,85], and the same spin/charge stripe structure [86–89]. At the particular 1/8 doping—due to phase competition—charge stripe order suppresses almost completely superconductivity. ARPES studies on these stripe ordered systems commonly report antinodal spectra with little low-energy spectral weight [39,41,90–92]. Different interpretations have been put forward [39,90]. In LBCO, it was suggested that the pseudogap (normal-state gap) has d -wave character and that the gap amplitude Δ is maximized at 1/8 doping [39] [this result is reproduced in Fig. 1(c)]. Subsequent experiments reported a correction to the d -wave symmetry [90]. This led to the

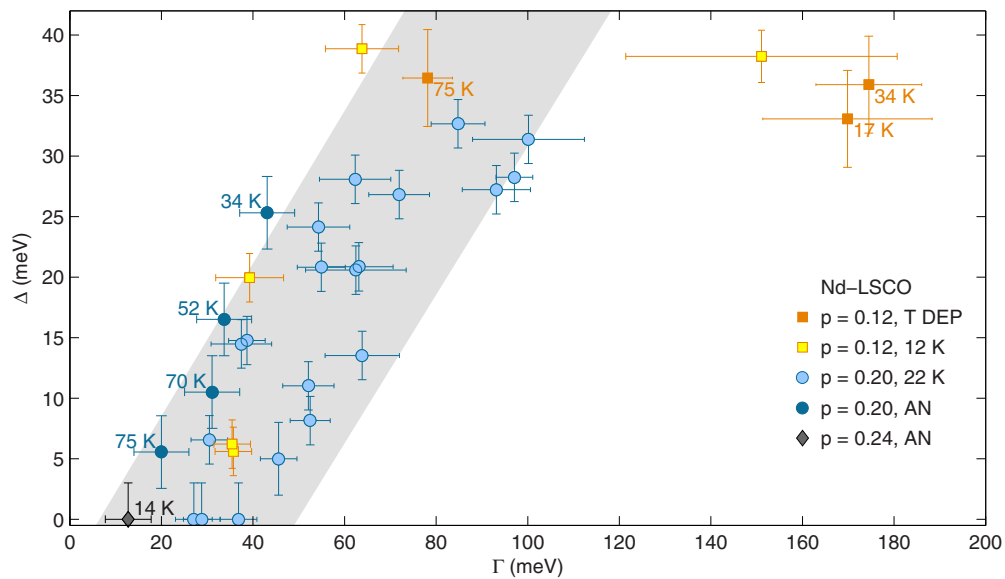


FIG. 5. (Color online) Normal-state gap Δ vs the scattering rate Γ . Both quantities were extracted by fitting background-subtracted symmetrized energy-distribution curves along the underlying Fermi surface of Nd-LSCO $p = 0.12, 0.20$, and 0.24 , as well as antinodal spectra vs temperature. The fitting procedure is explained in the text. Gray shaded area indicates schematically the correlation between the normal-state gap and the electron scattering.

proposal of a two-gap scenario [93–95], with an additional spectral gap (of unknown origin) in the antinodal region [90].

In Nd-LSCO $p = 0.12$, Fermi arcs with finite length were found even at the lowest measured temperatures [41]. To access the intrinsic spectral evolution as a function of momentum in Nd-LSCO $p = 0.12$, background-subtracted data should be considered. In Fig. 3(i), spectra near the antinodal region and close to the tip of the Fermi arc are compared. Near the tip, the spectrum resembles that observed in overdoped Nd-LSCO. Fitting to Eq. (2) yields $\Delta = 20 \pm 2$ meV and a scattering constant $\Gamma = 39 \pm 8$ meV. This is consistent with the approximate constant ratio of Δ / Γ (see Fig. 5) found for Nd-LSCO $p = 0.20$. The line shape of the antinodal spectra is, however, dramatically modified. A similar evolution was found in LBCO [90]. It seems that the system has lost coherence. Fitting using Eq. (2) indeed yields much smaller ratios of Δ / Γ —see Fig. 5. A sudden quasiparticle decoherence effect is therefore one possible explanation for the different antinodal line shape observed in the underdoped regime.

D. Effects of competing orders

Next, we discuss the possible influence of static long-range charge-density-wave order. For conventional CDW systems, the order parameter is identical to the single-particle gap [96], and Δ_{ch} scales with the lattice distortion u [96]. By measuring this distortion using hard x-ray diffraction, it was found that Δ_{ch} has a strong doping dependence [38] [reproduced in Fig. 1(b)]—peaking sharply at the 1/8 doping. Just a slight increase of doping, to say $p = 0.15$, results in a single-particle gap Δ_{ch} renormalized by a factor of five [38] (compared to 1/8 doping). Notice that the charge stripe onset temperature T_{ch} , observed by x-ray diffraction, varies more smoothly with doping. Hence, the coupling constant $\alpha = \Delta_{ch} / k_B T_{ch}$ has a strong doping dependence—being largest at 1/8 doping. It is also around this doping that quantum oscillation [97–100] and transport [23,84,101,102] experiments have revealed the Fermi-surface reconstruction in $\text{YBa}_2\text{Cu}_3\text{O}_y$ (YBCO) and $\text{HgBa}_2\text{CuO}_{4+\delta}$ (Hg1201). Charge ordering has been proposed as the mechanism responsible for this reconstruction [24,101]. Strongly coupled charge order is therefore not necessarily in contradiction with the observation of quasiparticles with light masses. Interestingly, neither the Fermi-surface reconstruction nor the effect of charge order have been convincingly probed by photoemission spectroscopy.

The observation of an electronic Fermi-surface reconstruction is complicated by orthorhombic distortions, which fold the bands similarly to what is expected from density-wave orders [103–105]. Moreover, identification of charge-density-wave order effects on the antinodal line shape in very underdoped compounds is complicated by superconductivity, pseudogaps, and possibly also spin-freezing phenomena [106,107]. The choice of Nd-LSCO, due to its low T_c , ensures that superconductivity is not influencing the problem. Furthermore, in this system, spin and charge-density-wave orderings are coupled [31], and hence part of the same phenomenon.

When a spectral gap Δ opens, low-energy spectral weight is either suppressed or redistributed in (k, ω) space. It has, for example, been shown that in Bi2212, pronounced redistribution of spectral weight—extending beyond 200 meV—appears

inside the pseudogap [76]. In Fig. 4(b), antinodal spectra of Nd-LSCO $p = 0.20$ display how the normal-state gap opens upon cooling. As the gap opens, spectral weight is transferred to larger energies, while the total amount of spectral weight remains approximately constant. This rearrangement of spectral weight manifests itself within an energy scale $(2 - 3)\Delta < 100$ meV. In the antinodal regime of stripe ordered Nd-LSCO $p = 0.12$, within the same temperature and energy window, the behavior is very different [see Fig. 4(a)]. Upon cooling, low-energy ($\omega < 100$ meV) spectral weight is removed with an apparent net loss of total weight. The k dependence in Figs. 3(c) and 3(i) does not suggest any pile up of spectral weight at other locations in momentum

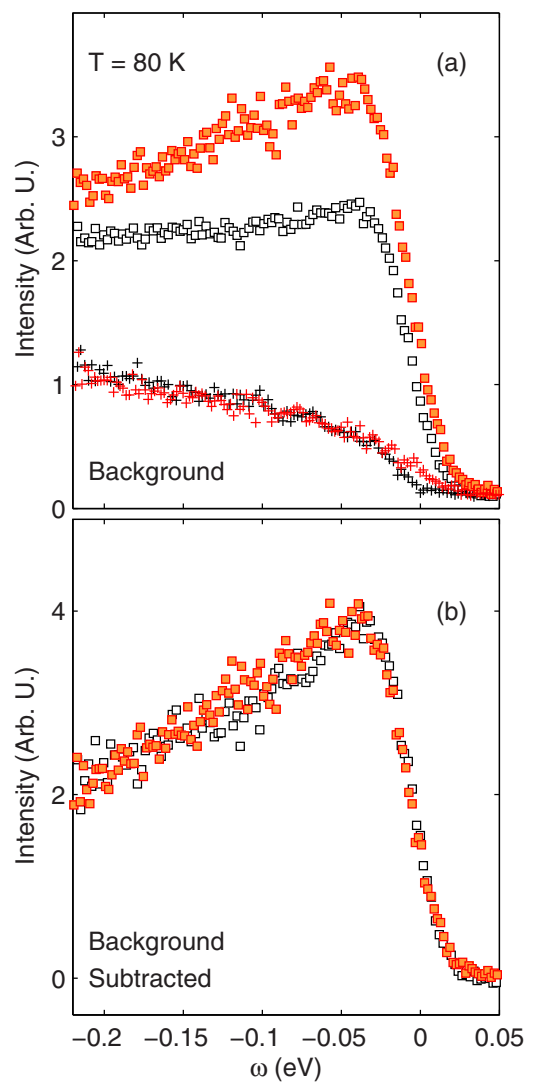


FIG. 6. (Color online) Comparison of antinodal spectra recorded on different surfaces of Nd-LSCO $p = 0.12$ at $T = 80$ K. (a) Raw spectra at k_F and at momentum k_{BG} , representing the extrinsic background. Intensities have been normalized so that the background intensities match across different experiments. In this fashion, it is shown how the same spectral line shape can appear different due to a different signal-to-background ratio. Spectra, at $T \sim 80$ K, were taken after cleaving at $T = 20$ K (black) and at 80 K (red). (b) Background-subtracted spectra, scaled by an arbitrary constant.

space. Thus either spectral weight is transferred to $\omega > 5\Delta$, or it is simply not conserved. A system that undergoes a phase transition may not display spectral weight conservation. Appearance of charge stripe order in the low-temperature tetragonal crystal structure may therefore lead to effective loss of spectral weight. In that case, stripe order seems to influence mainly the antinodal region and, remarkably, suppression of spectral weight extends up to energies as large as 100 meV.

V. CONCLUSIONS

In summary, we have presented a systematic angle-resolved photoemission spectroscopy, normal-state study of the charge stripe ordered cuprate compound $\text{La}_{1.6-x}\text{Nd}_{0.4}\text{Sr}_x\text{CuO}_4$ (Nd-LSCO). By varying the doping concentration, antinodal spectra were recorded from the overdoped metallic phase to the 1/8 doping—where static charge stripe order is stabilized. The metallic phase is characterized by gapless excitations even in the antinodal region. At $x = 0.20$, a spectral gap $\Delta \approx 30$ meV opens in the antinodal region but spectral weight remains conserved, although shifted to slightly larger energies. Analysis of the line shape suggests a correlation between electron scattering and the gap amplitude. Finally, for underdoped compounds, the antinodal line shape is quite different. Upon cooling into the stripe ordered phase, spectral weight appears to be lost. An additional source for spectral weight suppression is therefore proposed, and charge stripe order is discussed as an underlying mechanism.

ACKNOWLEDGMENTS

This work was supported by the Swiss National Science Foundation [through Grants No. 200020-105151, No. 200021-137783, No. 200020_159753/1, No. BSSGI0_155873 and its NCCR - MaNEP and Sinergia network Mott Physics Beyond the Heisenberg (HPBH) model], the Ministry of Education and Science of Japan, the United Kingdom Engineering and Physical Science Research Council [Grant No. EP/J015423/1],

Wenner-Gren Stiftelsen, and the Swedish Research Council. Work at ORNL was supported by the US Department of Energy, BES, Materials Sciences and Engineering Division. J.S.Z. and J.B.G. were supported by the US NSF (Grant No. DMR 1122603) and M.M. was supported by Marie Skłodowska Curie Action, International Career Grant through the European Union and Swedish Research Council (VR), Grant No. INCA-2014-6426. The photoemission experiments were performed at SLS of the Paul Scherrer Institut, Villigen PSI, Switzerland. We thank the X09LA beam-line [33] staff and Xiaoping Wang for technical support. We wish to thank Nicolas Doiron-Leyraud, Paul Freemann, Markus Hücker, Claude Monney, Henrik Rønnow, Louis Taillefer, and André-Marie Tremblay for enlightening discussions.

APPENDIX

All measured ARPES spectra contain background that typically vary slowly with momentum and excitation energy ω . The background can be evaluated at momenta far away from k_F . We found that across all dopings studied, the background has a very similar intensity profile as a function of ω . It is thus possible to scale ARPES intensities using this background. In Fig. 6, the background of two Nd-LSCO $p = 0.12$ antinodal spectra recorded under comparable conditions but on different surfaces is shown. The background can be scaled/normalized to give an essentially perfect match. Energy-distribution curves recorded at k_F are, however, displaying different intensities and line shapes. This demonstrates that from experiment to experiment, different signal-to-background ratios are observed. We stress that this effect is most visible at $p = 0.12$, where antinodal spectral weight appears strongly suppressed or redistributed. Once the background intensities are subtracted, the intrinsic line shape is essentially identical, irrespective of the signal-to-background ratio; see Fig. 6(b). Throughout this work, the detailed analysis of line shapes was carried out on the background-subtracted data.

-
- [1] N. Mannella, W. L. Yang, X. J. Zhou, H. Zheng, J. F. Mitchell, J. Zaanen, T. P. Devereaux, N. Nagaosa, Z. Hussain, and Z.-X. Shen, *Nature (London)* **438**, 474 (2005).
 - [2] S. V. Borisenko, A. A. Kordyuk, A. N. Yaresko, V. B. Zabolotnyy, D. S. Inosov, R. Schuster, B. Büchner, R. Weber, R. Follath, L. Patthey, and H. Berger, *Phys. Rev. Lett.* **100**, 196402 (2008).
 - [3] M. Uchida, K. Ishizaka, P. Hansmann, Y. Kaneko, Y. Ishida, X. Yang, R. Kumai, A. Toschi, Y. Onose, R. Arita, K. Held, O. K. Andersen, S. Shin, and Y. Tokura, *Phys. Rev. Lett.* **106**, 027001 (2011).
 - [4] M. Chand, G. Saraswat, A. Kamlapure, M. Mondal, S. Kumar, J. Jesudasan, V. Bagwe, L. Benfatto, V. Tripathi, and P. Raychaudhuri, *Phys. Rev. B* **85**, 014508 (2012).
 - [5] S. V. Borisenko, A. A. Kordyuk, V. B. Zabolotnyy, D. S. Inosov, D. Evtushinsky, B. Büchner, A. N. Yaresko, A. Varykhalov, R. Follath, W. Eberhardt, L. Patthey, and H. Berger, *Phys. Rev. Lett.* **102**, 166402 (2009).
 - [6] M. R. Norman, D. Pines, and C. Kallin, *Adv. Phys.* **54**, 715 (2005).
 - [7] U. Chatterjee, M. Shi, D. Ai, J. Zhao, A. Kanigel, S. Rosenkranz, H. Raffy, Z. Z. Li, K. Kadokawa, D. G. Hinks, Z. J. Xu7, J. S. Wen7, G. Gu, C. T. Lin, H. Claus, M. R. Norman, M. Randeria, and J. C. Campuzano, *Nat. Phys.* **6**, 99 (2010).
 - [8] J. Lee, K. Fujita, A. R. Schmidt, C. K. Kim, H. Eisaki, S. Uchida, and J. C. Davis, *Science* **325**, 1099 (2009).
 - [9] R. Daou, J. Chang, D. LeBoeuf, O. Cyr-Choinière, F. Laliberté, N. Doiron-Leyraud, B. J. Ramshaw, R. Liang, D. A. Bonn, W. N. Hardy, and L. Taillefer, *Nature (London)* **463**, 519 (2010).
 - [10] M. Hashimoto, R.-H. He, K. Tanaka, J.-P. Testaud, W. Meevasana, R. G. Moore, D. Lu, H. Yao, Y. Yoshida, H. Eisaki, T. P. Devereaux, Z. Hussain, and Z.-X. Shen, *Nat. Phys.* **6**, 414 (2010).
 - [11] T. Kondo, R. Khasanov, T. Takeuchi, J. Schmalian, and A. Kaminski, *Nature (London)* **457**, 296 (2009).

- [12] T. Kondo, Y. Hamaya, A. D. Palczewski, T. Takeuchi, J. S. Wen, Z. J. Xu, G. Gu, J. Schmalian, and A. Kaminski, *Nat. Phys.* **7**, 21 (2011).
- [13] T. Kondo, A. D. Palczewski, Y. Hamaya, T. Takeuchi, J. S. Wen, Z. J. Xu, G. Gu, and A. Kaminski, *Phys. Rev. Lett.* **111**, 157003 (2013).
- [14] S. Kawasaki, C. Lin, P. L. Kuhns, A. P. Reyes, and G.-q. Zheng, *Phys. Rev. Lett.* **105**, 137002 (2010).
- [15] Y. He, Y. Yin, M. Zech, A. Soumyanarayanan, M. M. Yee, T. Williams, M. C. Boyer, K. Chatterjee, W. D. Wise, I. Zeljkovic, T. Kondo, T. Takeuchi, H. Ikuta, P. Mistark, R. S. Markiewicz, A. Bansil, S. Sachdev, E. W. Hudson, and J. E. Hoffman, *Science* **344**, 608 (2014).
- [16] T. Wu, H. Mayaffre, S. Krämer, M. Horvatic, C. Berthier, W. N. Hardy, R. Liang, D. A. Bonn, and M.-H. Julien, *Nature (London)* **477**, 191 (2011).
- [17] T. Wu, H. Mayaffre, S. Krämer, M. Horvatić, C. Berthier, P. L. Kuhns, A. P. Reyes, R. Liang, W. N. Hardy, D. A. Bonn, and M.-H. Julien, *Nat. Commun.* **4**, 2113 (2013).
- [18] J. Chang, E. Blackburn, A. T. Holmes, N. B. Christensen, J. Larsen, J. Mesot, R. Liang, D. A. Bonn, W. N. Hardy, A. Watenphul, M. v. Zimmermann, E. M. Forgan, and S. M. Hayden, *Nat. Phys.* **8**, 871 (2012).
- [19] G. Ghiringhelli, M. Le Tacon, M. Minola, S. Blanco-Canosa, C. Mazzoli, N. B. Brookes, G. M. De Luca, A. Frano, D. G. Hawthorn, F. He, T. Loew, M. M. Sala, D. C. Peets, M. Salluzzo, E. Schierle, R. Sutarto, G. A. Sawatzky, E. Weschke, B. Keimer, and L. Braicovich, *Science* **337**, 821 (2012).
- [20] A. J. Achkar, R. Sutarto, X. Mao, F. He, A. Frano, S. Blanco-Canosa, M. Le Tacon, G. Ghiringhelli, L. Braicovich, M. Minola, M. Moretti Sala, C. Mazzoli, R. Liang, D. A. Bonn, W. N. Hardy, B. Keimer, G. A. Sawatzky, and D. G. Hawthorn, *Phys. Rev. Lett.* **109**, 167001 (2012).
- [21] M. Hücker, N. B. Christensen, A. T. Holmes, E. Blackburn, E. M. Forgan, R. Liang, D. A. Bonn, W. N. Hardy, O. Gutowski, M. v. Zimmermann, S. M. Hayden, and J. Chang, *Phys. Rev. B* **90**, 054514 (2014).
- [22] S. Blanco-Canosa, A. Frano, E. Schierle, J. Porras, T. Loew, M. Minola, M. Bluschke, E. Weschke, B. Keimer, and M. Le Tacon, *Phys. Rev. B* **90**, 054513 (2014).
- [23] N. Doiron-Leyraud, S. Lepault, O. Cyr-Choinière, B. Vignolle, G. Grissonnanche, F. Laliberté, J. Chang, N. Barišić, M. K. Chan, L. Ji, X. Zhao, Y. Li, M. Greven, C. Proust, and L. Taillefer, *Phys. Rev. X* **3**, 021019 (2013).
- [24] W. Tabis, Y. Li, M. L. Tacon, L. Braicovich, A. Kreyssig, M. Minola, G. Dellea, E. Weschke, M. J. Veit, M. Ramazanoglu, A. I. Goldman, T. Schmitt, G. Ghiringhelli, N. Barić, M. K. Chan, C. J. Dorow, G. Yu, X. Zhao, B. Keimer, and M. Greven, *Nat. Commun.* **5**, 5875 (2014).
- [25] E. H. da Silva Neto, P. Aynajian, A. Frano, R. Comin, E. Schierle, E. Weschke, A. Gyenis, J. Wen, J. Schneeloch, Z. Xu, S. Ono, G. Gu, M. Le Tacon, and A. Yazdani, *Science* **343**, 393 (2014).
- [26] R. Comin, A. Frano, M. M. Yee, Y. Yoshida, H. Eisaki, E. Schierle, E. Weschke, R. Sutarto, F. He, A. Soumyanarayanan, Y. He, M. Le Tacon, I. S. Elfimov, J. E. Hoffman, G. A. Sawatzky, B. Keimer, and A. Damascelli, *Science* **343**, 390 (2014).
- [27] K. Fujita, C. K. Kim, I. Lee, J. Lee, M. H. Hamidian, I. A. Firso, S. Mukhopadhyay, H. Eisaki, S. Uchida, M. J. Lawler, E.-A. Kim, and J. C. Davis, *Science* **344**, 612 (2014).
- [28] N. B. Christensen, J. Chang, J. Larsen, M. Fujita, M. Oda, M. Ido, N. Momono, E. M. Forgan, A. T. Holmes, J. Mesot, M. Huecker, and M. v. Zimmermann, *arXiv:1404.3192*.
- [29] V. Thampy, M. P. M. Dean, N. B. Christensen, L. Steinke, Z. Islam, M. Oda, M. Ido, N. Momono, S. B. Wilkins, and J. P. Hill, *Phys. Rev. B* **90**, 100510 (2014).
- [30] T. P. Croft, C. Lester, M. S. Senn, A. Bombardi, and S. M. Hayden, *Phys. Rev. B* **89**, 224513 (2014).
- [31] J. M. Tranquada, B. J. Sternlieb, J. D. Axe, Y. Nakamura, and S. Uchida, *Nature (London)* **375**, 561 (1995).
- [32] N. B. Christensen, H. M. Rønnow, J. Mesot, R. A. Ewings, N. Momono, M. Oda, M. Ido, M. Enderle, D. F. McMorrow, and A. T. Boothroyd, *Phys. Rev. Lett.* **98**, 197003 (2007).
- [33] U. Flechsig, L. Patthey, and T. Schmidt, *AIP Conf. Proc.* **705**, 316 (2004).
- [34] R. Daou, N. Doiron-Leyraud, D. LeBoeuf, S. Y. Li, F. Laliberté, O. Cyr-Choinière, Y. J. Jo, L. Balicas, J.-Q. Yan, J.-S. Zhou, J. B. Goodenough, and L. Taillefer, *Nat. Phys.* **5**, 31 (2009).
- [35] O. Cyr-Choinière, R. Daou, J. Chang, F. Laliberté, N. Doiron-Leyraud, D. LeBoeuf, Y. Jo, L. Balicas, J.-Q. Yan, J.-G. Cheng, J.-S. Zhou, J. Goodenough, and L. Taillefer, *Physica C* **470**, Suppl. 1, S12 (2010).
- [36] S. Wakimoto, R. J. Birgeneau, Y. Fujimaki, N. Ichikawa, T. Kasuga, Y. J. Kim, K. M. Kojima, S.-H. Lee, H. Niko, J. M. Tranquada, S. Uchida, and M. v. Zimmermann, *Phys. Rev. B* **67**, 184419 (2003).
- [37] J. Fink, V. Soltwisch, J. Geck, E. Schierle, E. Weschke, and B. Büchner, *Phys. Rev. B* **83**, 092503 (2011).
- [38] M. Hücker, M. v. Zimmermann, Z. J. Xu, J. S. Wen, G. D. Gu, and J. M. Tranquada, *Phys. Rev. B* **87**, 014501 (2013).
- [39] T. Valla, A. V. Fedorov, J. Lee, J. C. Davis, and G. D. Gu, *Science* **314**, 1914 (2006).
- [40] M. Måansson, T. Claesson, U. O. Karlsson, O. Tjernberg, S. Pailhs, J. Chang, J. Mesot, M. Shi, L. Patthey, N. Momono, M. Oda, and M. Ido, *Rev. Sci. Instrum.* **78**, 076103 (2007).
- [41] J. Chang, Y. Sassa, S. Guerrero, M. Måansson, M. Shi, S. Pailhés, A. Bendounan, R. Mottl, T. Claesson, O. Tjernberg, L. Patthey, M. Ido, M. Oda, N. Momono, C. Mudry, and J. Mesot, *New J. Phys.* **10**, 103016 (2008).
- [42] T. Claesson, M. Måansson, A. Önstens, M. Shi, Y. Sassa, S. Pailhés, J. Chang, A. Bendounan, L. Patthey, J. Mesot, T. Muro, T. Matsushita, T. Kinoshita, T. Nakamura, N. Momono, M. Oda, M. Ido, and O. Tjernberg, *Phys. Rev. B* **80**, 094503 (2009).
- [43] T. Yoshida, X. J. Zhou, K. Tanaka, W. L. Yang, Z. Hussain, Z.-X. Shen, A. Fujimori, S. Sahrakorpi, M. Lindroos, R. S. Markiewicz, A. Bansil, S. Komiya, Y. Ando, H. Eisaki, T. Kakeshita, and S. Uchida, *Phys. Rev. B* **74**, 224510 (2006).
- [44] E. Razzoli, Y. Sassa, G. Drachuck, M. Måansson, A. Keren, M. Shay, M. H. Berntsen, O. Tjernberg, M. Radovic, J. Chang, S. Pailhés, N. Momono, M. Oda, M. Ido, O. J. Lipscombe, S. M. Hayden, L. Patthey, J. Mesot, and M. Shi, *New J. Phys.* **12**, 125003 (2010).
- [45] A. Kaminski, S. Rosenkranz, H. M. Fretwell, M. R. Norman, M. Randeria, J. C. Campuzano, J.-M. Park, Z. Z. Li, and H. Raffy, *Phys. Rev. B* **73**, 174511 (2006).

- [46] S. Benhabib, A. Sacuto, M. Civelli, I. Paul, M. Cazayous, Y. Gallais, M.-A. Méasson, R. D. Zhong, J. Schneeloch, G. D. Gu, D. Colson, and A. Forget, *Phys. Rev. Lett.* **114**, 147001 (2015).
- [47] M. R. Norman, H. Ding, M. Randeria, J. C. Campuzano, T. Yokoya, T. Takeuchi, T. Takahashi, T. Mochiku, K. Kadokawa, P. Guptasarma, and D. G. Hinks, *Nature (London)* **392**, 157 (1998).
- [48] M. Hashimoto, I. M. Vishik, R.-H. He, T. P. Devereaux, and Z.-X. Shen, *Nat. Phys.* **10**, 483 (2014).
- [49] U. Chatterjee, D. Ai, J. Zhao, S. Rosenkranz, A. Kaminski, H. Raffy, Z. Li, K. Kadokawa, M. Randeria, M. R. Norman, and J. C. Campuzano, *Proc. Natl. Acad. Sci. USA* **108**, 9346 (2011).
- [50] K. Tanaka, W. S. Lee, D. H. Lu, A. Fujimori, T. Fujii, Risdiana, I. Terasaki, D. J. Scalapino, T. P. Devereaux, Z. Hussain, and Z.-X. Shen, *Science* **314**, 1910 (2006).
- [51] M. Shi, J. Chang, S. Pailhés, M. R. Norman, J. C. Campuzano, M. Måansson, T. Claesson, O. Tjernberg, A. Bendounan, L. Patthey, N. Momono, M. Oda, M. Ido, C. Mudry, and J. Mesot, *Phys. Rev. Lett.* **101**, 047002 (2008).
- [52] M. Shi, A. Bendounan, E. Razzoli, S. Rosenkranz, M. R. Norman, J. C. Campuzano, J. Chang, M. Mnsson, Y. Sassa, T. Claesson, O. Tjernberg, L. Patthey, N. Momono, M. Oda, M. Ido, S. Guerrero, C. Mudry, and J. Mesot, *Europhys. Lett.* **88**, 27008 (2009).
- [53] J. Chang, M. Shi, S. Pailhés, M. Måansson, T. Claesson, O. Tjernberg, A. Bendounan, Y. Sassa, L. Patthey, N. Momono, M. Oda, M. Ido, S. Guerrero, C. Mudry, and J. Mesot, *Phys. Rev. B* **78**, 205103 (2008).
- [54] J. Chang, A. P. Schnyder, R. Gilardi, H. M. Rønnow, S. Pailhes, N. B. Christensen, C. Niedermayer, D. F. McMorrow, A. Hiess, A. Stunault, M. Enderle, B. Lake, O. Sobolev, N. Momono, M. Oda, M. Ido, C. Mudry, and J. Mesot, *Phys. Rev. Lett.* **98**, 077004 (2007).
- [55] J. Chang, C. Niedermayer, R. Gilardi, N. B. Christensen, H. M. Rønnow, D. F. McMorrow, M. Ay, J. Stahn, O. Sobolev, A. Hiess, S. Pailhes, C. Baines, N. Momono, M. Oda, M. Ido, and J. Mesot, *Phys. Rev. B* **78**, 104525 (2008).
- [56] J. Chang, J. S. White, M. Laver, C. J. Bowell, S. P. Brown, A. T. Holmes, L. Maechler, S. Strässle, R. Gilardi, S. Gerber, T. Kurosawa, N. Momono, M. Oda, M. Ido, O. J. Lipscombe, S. M. Hayden, C. D. Dewhurst, R. Vavrin, J. Gavilano, J. Kohlbrecher, E. M. Forgan, and J. Mesot, *Phys. Rev. B* **85**, 134520 (2012).
- [57] A. V. Chubukov, M. R. Norman, A. J. Millis, and E. Abrahams, *Phys. Rev. B* **76**, 180501 (2007).
- [58] A. Kanigel, M. R. Norman, M. Randeria, U. Chatterjee, S. Souma, A. Kaminski, H. M. Fretwell, S. Rosenkranz, M. Shi, T. Sato, T. Takahashi, Z. Z. Li, H. Raffy, K. Kadokawa, D. Hinks, L. Ozyuzer, and J. C. Campuzano, *Nat. Phys.* **2**, 447 (2006).
- [59] M. R. Norman, M. Randeria, H. Ding, and J. C. Campuzano, *Phys. Rev. B* **57**, R11093 (1998).
- [60] M. Franz and A. J. Millis, *Phys. Rev. B* **58**, 14572 (1998).
- [61] G.-H. Gweon, B. S. Shastry, and G. D. Gu, *Phys. Rev. Lett.* **107**, 056404 (2011).
- [62] C. G. Fatuzzo, Y. Sassa, M. Måansson, S. Pailhès, O. J. Lipscombe, S. M. Hayden, L. Patthey, M. Shi, M. Grioni, H. M. Rønnow, J. Mesot, O. Tjernberg, and J. Chang, *Phys. Rev. B* **89**, 205104 (2014).
- [63] T. Valla, A. V. Fedorov, P. D. Johnson, Q. Li, G. D. Gu, and N. Koshizuka, *Phys. Rev. Lett.* **85**, 828 (2000).
- [64] J. Chang, M. Måansson, S. Pailhès, T. Claesson, O. J. Lipscombe, S. M. Hayden, L. Patthey, O. Tjernberg, and J. Mesot, *Nat. Commun.* **4**, 2559 (2013).
- [65] J. W. Alldredge, J. Lee, K. McElroy, M. Wang, K. Fujita, Y. Kohsaka, C. Taylor, H. Eisaki, S. Uchida, P. J. Hirschfeld, and J. C. Davis, *Nat. Phys.* **4**, 319 (2008).
- [66] T. Kato, T. Maruyama, S. Okitsu, and H. Sakata, *J. Phys. Soc. Jpn.* **77**, 054710 (2008).
- [67] A. Kaminski, H. M. Fretwell, M. R. Norman, M. Randeria, S. Rosenkranz, U. Chatterjee, J. C. Campuzano, J. Mesot, T. Sato, T. Takahashi, T. Terashima, M. Takano, K. Kadokawa, Z. Z. Li, and H. Raffy, *Phys. Rev. B* **71**, 014517 (2005).
- [68] D. Sénéchal and A.-M. S. Tremblay, *Phys. Rev. Lett.* **92**, 126401 (2004).
- [69] E. Gull, O. Parcollet, and A. J. Millis, *Phys. Rev. Lett.* **110**, 216405 (2013).
- [70] G. Sordi, P. Sémond, K. Haule, and A.-M. S. Tremblay, *Phys. Rev. B* **87**, 041101 (2013).
- [71] M. Ferrero, P. S. Cornaglia, L. D. Leo, O. Parcollet, G. Kotliar, and A. Georges, *Europhys. Lett.* **85**, 57009 (2009).
- [72] H. Alloul, *C. R. Phys.* **15**, 519 (2014).
- [73] P. A. Lee, *Phys. Rev. X* **4**, 031017 (2014).
- [74] I. M. Vishik, M. Hashimoto, R.-H. He, W.-S. Lee, F. Schmitt, D. Lu, R. G. Moore, C. Zhang, W. Meevasan, T. Sasagawa, S. Uchida, K. Fujita, S. Ishida, M. Ishikado, Y. Yoshida, H. Eisaki, Z. Hussain, T. P. Devereaux, and Z.-X. Shen, *Proc. Natl. Acad. Sci. USA* **109**, 18332 (2012).
- [75] E. G. Moon and S. Sachdev, *Phys. Rev. B* **82**, 104516 (2010).
- [76] M. Hashimoto, E. A. Nowadnick, R.-H. He, I. M. Vishik, B. Moritz, Y. He, K. Tanaka, R. G. Moore, D. Lu, Y. Yoshida, M. Ishikado, T. Sasagawa, K. Fujita, S. Ishida, S. Uchida, H. Eisaki, Z. Hussain, T. P. Devereaux, and Z.-X. Shen, *Nat. Mater.* **14**, 37 (2015).
- [77] A. Greco, *Phys. Rev. Lett.* **103**, 217001 (2009).
- [78] A. Greco and M. Bejas, *Phys. Rev. B* **83**, 212503 (2011).
- [79] C. Monney, G. Monney, P. Aebi, and H. Beck, *Phys. Rev. B* **85**, 235150 (2012).
- [80] D. S. Inosov, D. V. Evtushinsky, V. B. Zabolotnyy, A. A. Kordyuk, B. Büchner, R. Follath, H. Berger, and S. V. Borisenko, *Phys. Rev. B* **79**, 125112 (2009).
- [81] T. Kiss, T. Yokoya, A. Chainani, S. Shin, T. Hanaguri, M. Nohara, and H. Takagi, *Nat. Phys.* **3**, 720 (2007).
- [82] U. Chatterjee, J. Zhao, M. Iavarone, R. Di Capua, J. P. Castellan, G. Karapetrov, C. D. Malliakas, M. G. Kanatzidis, H. Claus, J. P. C. Ruff, F. Weber, J. van Wezel, J. C. Campuzano, R. Osborn, M. Randeria, N. Trivedi, M. R. Norman, and S. Rosenkranz, *Nat. Commun.* **6**, 6313 (2015).
- [83] M. Vojta, *Adv. Phys.* **58**, 699 (2009).
- [84] J. Chang, R. Daou, C. Proust, D. LeBoeuf, N. Doiron-Leyraud, F. Laliberté, B. Pingault, B. J. Ramshaw, R. Liang, D. A. Bonn, W. N. Hardy, H. Takagi, A. B. Antunes, I. Sheikin, K. Behnia, and L. Taillefer, *Phys. Rev. Lett.* **104**, 057005 (2010).
- [85] Q. Li, M. Hücker, G. D. Gu, A. M. Tsvelik, and J. M. Tranquada, *Phys. Rev. Lett.* **99**, 067001 (2007).
- [86] S. B. Wilkins, M. P. M. Dean, J. Fink, M. Hücker, J. Geck, V. Soltwisch, E. Schierle, E. Weschke, G. Gu, S. Uchida, N.

- [87] Ichikawa, J. M. Tranquada, and J. P. Hill, *Phys. Rev. B* **84**, 195101 (2011).
- [87] B. Nachumi, Y. Fudamoto, A. Keren, K. M. Kojima, M. Larkin, G. M. Luke, J. Merrin, O. Tchernyshyov, Y. J. Uemura, N. Ichikawa, M. Goto, H. Takagi, S. Uchida, M. K. Crawford, E. M. McCarron, D. E. MacLaughlin, and R. H. Heffner, *Phys. Rev. B* **58**, 8760 (1998).
- [88] J. M. Tranquada, J. D. Axe, N. Ichikawa, Y. Nakamura, S. Uchida, and B. Nachumi, *Phys. Rev. B* **54**, 7489 (1996).
- [89] M. Fujita, H. Goka, K. Yamada, J. M. Tranquada, and L. P. Regnault, *Phys. Rev. B* **70**, 104517 (2004).
- [90] R.-H. He, K. Tanaka, S.-K. Mo, T. Sasagawa, M. Fujita, T. Adachi, N. Mannella, K. Yamada, Y. Koike, Z. Hussain, and Z.-X. Shen, *Nat. Phys.* **5**, 119 (2009).
- [91] V. B. Zabolotnyy, A. A. Kordyuk, D. S. Inosov, D. V. Evtushinsky, R. Schuster, B. Bchner, N. Wizent, G. Behr, S. Pyon, T. Takayama, H. Takagi, R. Follath, and S. V. Borisenko, *Europhys. Lett.* **86**, 47005 (2009).
- [92] T. Valla, *Physica C* **481**, 66 (2012).
- [93] T. Kondo, T. Takeuchi, A. Kaminski, S. Tsuda, and S. Shin, *Phys. Rev. Lett.* **98**, 267004 (2007).
- [94] S. Hüfner, M. A. Hossain, A. sscelli, and G. A. Sawatzky, *Rep. Prog. Phys.* **71**, 062501 (2008).
- [95] J.-H. Ma, Z.-H. Pan, F. C. Niestemski, M. Neupane, Y.-M. Xu, P. Richard, K. Nakayama, T. Sato, T. Takahashi, H.-Q. Luo, L. Fang, H.-H. Wen, Z. Wang, H. Ding, and V. Madhavan, *Phys. Rev. Lett.* **101**, 207002 (2008).
- [96] G. Grüner, *Rev. Mod. Phys.* **60**, 1129 (1988).
- [97] N. Doiron-Leyraud, C. Proust, D. LeBoeuf, J. Levallois, J.-B. Bonnemaison, R. Liang, D. A. Bonn, W. N. Hardy, and L. Taillefer, *Nature (London)* **447**, 565 (2007).
- [98] S. E. Sebastian, N. Harrison, and G. G. Lonzarich, *Rep. Prog. Phys.* **75**, 102501 (2012).
- [99] B. Vignolle, D. Vignolles, D. LeBoeuf, S. Lepault, B. Ramshaw, R. Liang, D. Bonn, W. Hardy, N. Doiron-Leyraud, A. Carrington, N. Hussey, L. Taillefer, and C. Proust, *C. R. Phys.* **12**, 446 (2011).
- [100] N. Barišić, S. Badoux, M. K. Chan, C. Dorow, W. Tabis, B. Vignolle, G. Yu, J. Béard, X. Zhao, C. Proust, and M. Greven, *Nat. Phys.* **9**, 761 (2013).
- [101] F. Laliberté, J. Chang, N. Doiron-Leyraud, E. Hassinger, R. Daou, M. Rondeau, B. Ramshaw, R. Liang, D. Bonn, W. Hardy, S. Pyon, T. Takayama, H. Takagi, I. Sheikin, L. Malone, C. Proust, K. Behnia, and L. Taillefer, *Nat. Commun.* **2**, 432 (2011).
- [102] D. LeBoeuf, N. Doiron-Leyraud, B. Vignolle, M. Sutherland, B. J. Ramshaw, J. Levallois, R. Daou, F. Laliberté, O. Cyr-Choinière, J. Chang, Y. J. Jo, L. Balicas, R. Liang, D. A. Bonn, W. N. Hardy, C. Proust, and L. Taillefer, *Phys. Rev. B* **83**, 054506 (2011).
- [103] R.-H. He, X. J. Zhou, M. Hashimoto, T. Yoshida, K. Tanaka, S.-K. Mo, T. Sasagawa, N. Mannella, W. Meevasana, H. Yao, M. Fujita, T. Adachi, S. Komiya, S. Uchida, Y. Ando, F. Zhou, Z. X. Zhao, A. Fujimori, Y. Koike, K. Yamada, Z. Hussain, and Z.-X. Shen, *New J. Phys.* **13**, 013031 (2011).
- [104] J. Meng, G. Liu, W. Zhang, L. Zhao, H. Liu, X. Jia, D. Mu, S. Liu, X. Dong, J. Zhang, W. Lu, G. Wang, Y. Zhou, Y. Zhu, X. Wang, Z. Xu, C. Chen, and X. J. Zhou, *Nature (London)* **462**, 335 (2009).
- [105] P. D. C. King, J. A. Rosen, W. Meevasana, A. Tamai, E. Rozbicki, R. Comin, G. Levy, D. Fournier, Y. Yoshida, H. Eisaki, K. M. Shen, N. J. C. Ingle, A. Damascelli, and F. Baumberger, *Phys. Rev. Lett.* **106**, 127005 (2011).
- [106] M. Fujita, K. Yamada, H. Hiraka, P. M. Gehring, S. H. Lee, S. Wakimoto, and G. Shirane, *Phys. Rev. B* **65**, 064505 (2002).
- [107] S. Wakimoto, S. Ueki, Y. Endoh, and K. Yamada, *Phys. Rev. B* **62**, 3547 (2000).